Laser spectroscopy of crossed molecular beams: The dissociation energy of BaI from energy-balance measurements

P. H. Vaccaro,[a] D. Zhao, A. A. Tsekouras, C. A. Leach,[b] W. E. Ernst,[c] and R. N. Zare[d]
Department of Chemistry, Stanford University, Stanford, California 94305-5080

(Received 30 August 1990; accepted 13 September 1990)

Through application of energy-balance arguments to the crossed-beam reaction $Ba(^1S_0) + HI(X\,^1\Sigma^+) \rightarrow BaI(X\,^2\Sigma^+) + H(^2S_{1/2})$, a lower limit for the BaI bond dissociation energy is determined to be $D_0^0(BaI) \gtrsim 76.8 \pm 1.7$ kcal/mol (3.33 ± 0.07 eV). Based on the upper bound of $D_0^0(BaI) \lesssim 78.5 \pm 0.5$ kcal/mol, as determined from earlier predissociation studies [M. A. Johnson, J. Allison, and R. N. Zare, J. Chem. Phys. **85**, 5723 (1986)], we recommend a BaI bond strength of 77.7 ± 2.0 kcal/mol (3.37 ± 0.09 eV). This dissociation energy is more than 5 kcal/mol higher than the previously accepted value of $D_0^0(BaI)$ as derived from mass spectrometric measurements.

I. INTRODUCTION

Bond strengths are traditionally determined from thermodynamic studies based either on the measurement of equilibrium constant variations as a function of temperature or on the application of Hess' law to a closed cycle of chemical transformations.[1] An alternative method, which has met with only meager success and has often led to quite misleading conclusions, entails extrapolation of spectroscopic data to the asymptotic limit of bond dissociation.[1] With developments in molecular beam techniques and laser spectroscopy, bond strengths deduced from the application of energy conservation criteria to the nascent products of isolated chemical reactions have become available.[2] Unfortunately, this latter method has seldom been used effectively because of difficulties involved in eliminating secondary processes (e.g., collisional relaxation) and in providing well-defined initial reaction conditions. However, when feasible, such energy-balance studies should result in bond strengths limited in accuracy only by how well the spectroscopy and the recoil energy of the product molecules are known.

In this paper, we report a new measurement for the bond dissociation energy of BaI based on the reaction

$$Ba(^1S_0) + HI(X\,^1\Sigma^+) \rightarrow BaI(X\,^2\Sigma^+) + H(^2S_{1/2}), \quad (1)$$

where all species are in their ground electronic states. Although the main thrust of our research efforts has been elucidation of the detailed relationship between reagent impact parameters and final product states,[3] the value of $D_0^0(BaI)$ is of fundamental importance for the interpretation of dynamical processes exhibited by the Ba + HI reaction system. The present investigation entailed formation of $BaI(X\,^2\Sigma^+)$ under the well-defined, single-collision conditions afforded by crossed-beam techniques and subsequent examination of internal state distributions in the nascent product molecules via high-resolution laser-induced fluorescence (LIF) spectroscopy. Application of energy conservation arguments to our measurements enabled a lower bound for the bond strength of BaI to be obtained.

Despite considerable efforts by numerous research groups, the bond dissociation energy of BaI has remained a matter of considerable speculation and contention. Early calculations, based on variations of the Rittner ionic model,[4] indicated a value of 85 ± 15 kcal/mol.[5] By analyzing BaI product angular distributions arising from the effusive crossed-beam reaction of Ba with HI, Mims, Lin, and Herm[6] established a rigorous lower bound for $D_0^0(BaI)$ of 66 kcal/mol. A subsequent study of chemiluminescence produced by the formation of electronically excited BaI in the Ba + I_2[7] reaction system suggested that the bond strength of BaI lies in the vicinity of 100 kcal/mol. Unfortunately, the results derived from this study must be disregarded due to probable contamination of the presumed ground state barium source by metastable $Ba(^3D)$ atoms.[8]

Kleinschmidt and Hildenbrand have applied the techniques of mass spectrometry to the determination of BaI dissociation energies.[9] Their study entailed the measurement of equilibrium compositions for effusive beams containing BaI molecules formed from the high-temperature (1500–1900 K) reaction of BaO with HI. Careful analysis of the resulting thermochemical data yielded $D_0^0(BaI) = 71.4 \pm 1.0$ kcal/mol, a value in good agreement with that suggested by extrapolating experimental bond strengths from the other barium monohalides.[10]

Exploiting their ability to generate metastable barium atoms, Estler and Zare[8] have reinvestigated the Ba + I_2 reaction system so as to determine a new value for $D_0^0(BaI)$. Spectral dispersion of chemiluminescence from electronically excited BaI formed under single-collision beam-gas conditions enabled the internal state distributions for nascent product molecules to be examined. With the initial relative translational energy of the reagents derived via a novel time-

[a] Present address: Department of Chemistry, Yale University, New Haven, CT 06511.
[b] Née Montgomerie
[c] Present address: Department of Physics, 104 Davey Laboratory, Pennsylvania State University, University Park, PA 16802.
[d] Author to whom correspondence should be addressed.

 0021-9606/90/248544-13$03.00

of-flight technique, these authors were able to apply energy conservation criteria to yield a lower limit of 72.9 ± 2 kcal/mol for the bond strength of BaI. While not inconsistent with the results reported by Kleinschmidt and Hildenbrand,[9] this value of $D_0^0(\mathrm{BaI})$ still seems to be somewhat low, given the wide distribution of BaI product states observed in other beam-gas reactive studies.[11,12]

In a recent study of BaI product state distributions resulting from the beam-gas reaction of $\mathrm{Ba}(^1S_0)$ with CF_3I, Johnson, Allison, and Zare[13] have been able to establish a purely spectroscopic upper bound for the bond dissociation energy of BaI. Based on evidence for the onset of predissociation in the BaI $C\,^2\Pi$ excited electronic state, believed to be induced by repulsive curves correlating to the same asymptotic separated-atom limit as the BaI $X\,^2\Sigma^+$ ground state, these authors have concluded that $D_0^0(\mathrm{BaI}) \lesssim 78.5 \pm 0.5$ kcal/mol. With almost 6 kcal/mol separating this rigorous upper bound from the lower limit reported by Estler and Zare,[8] a new, more accurate experimental measurement of the bond strength for BaI would be most welcome. In particular, this wide range of possible values for $D_0^0(\mathrm{BaI})$ has been a vexing problem for the detailed interpretation of reaction dynamics in the $\mathrm{Ba} + \mathrm{HI}$,[11,14,15] $\mathrm{Ba} + CH_3I$,[12,16] $\mathrm{Ba} + CH_2I_2$,[12] and $\mathrm{Ba} + CF_3I$[13,16,17] systems.

The experimental scheme utilized for the present determination of $D_0^0(\mathrm{BaI})$ has several distinct advantages over those employed in previous studies. In particular, our use of a crossed-beam reaction apparatus, in which "effusive" $\mathrm{Ba}(^1S_0)$ and supersonic $\mathrm{HI}(X\,^1\Sigma^+)$ beams interacted under single-collision conditions, enabled well-defined, controllable distributions of relative reagent velocities to be prepared while simultaneously ensuring that observed product molecules were in an unrelaxed, nascent state. Compared to more conventional bulk gas or beam-gas measurements, the narrow spread in reactant translational energy afforded by the crossed-beam technique greatly enhanced the reliability and precision of energy balance arguments as applied to the evaluation of $D_0^0(\mathrm{BaI})$.

The LIF product detection scheme exploited in the present work permits the partitioning of internal energy within the BaI product to be precisely determined. Previous attempts to determine $D_0^0(\mathrm{BaI})$ with optical spectroscopic probes have relied on measurements made via low-resolution dispersed chemiluminescence,[7,8] or through LIF excited by large-bandwidth pulsed lasers.[13] In contrast, our use of a frequency- and power-stabilized, single-mode excitation source enables identification of individual rovibronic transitions within the exceptionally congested LIF spectrum of BaI.[18,19] From the viewpoint of $D_0^0(\mathrm{BaI})$ measurements, this high-resolution capability is essential for the observation and assignment of spectral features corresponding to the population of internal product states up to the limit imposed by conservation of total available energy.

The following section provides a brief review of the energy-balance arguments required for determination of bond strengths from the spectroscopic analysis of nascent product molecules. A detailed description of experimental techniques employed for investigation of the $\mathrm{Ba} + \mathrm{HI}$ reaction system will be subsequently presented. Finally, the results derived from our measurements will be discussed and compared with the values for $D_0^0(\mathrm{BaI})$ reported by previous studies. A recommended value of the bond strength of BaI, obtained from experimentally determined upper and lower bounds for $D_0^0(\mathrm{BaI})$, will be suggested.

II. METHODOLOGY

The present determination of $D_0^0(\mathrm{BaI})$ is based upon the application of energy conservation principles to the closed reaction system of Eq. (1). This required that the total energy for the reagents

$$E_{\mathrm{reag}} = E_{\mathrm{rel}}(\mathrm{Ba} - \mathrm{HI}) + E_{\mathrm{int}}(\mathrm{Ba}) + E_{\mathrm{int}}(\mathrm{HI}) - D_0^0(\mathrm{HI}) \tag{2}$$

be equated to that of the products

$$E_{\mathrm{prod}} = E_{\mathrm{rel}}(\mathrm{BaI} - \mathrm{H}) + E_{\mathrm{int}}(\mathrm{H}) + E_{\mathrm{int}}(\mathrm{BaI}) - D_0^0(\mathrm{BaI}), \tag{3}$$

where E_{rel} and E_{int} denote the energy associated with translational and internal degrees of freedom, respectively. For two interacting particles $A + BC$, the corresponding relative translational energy in the center-of-mass frame $E_{\mathrm{rel}}(A - BC)$ can readily be expressed[20] in terms of the appropriate reduced mass μ_{A-BC} and relative velocity $v_{\mathrm{rel}}(A - BC)$, such that

$$E_{\mathrm{rel}}(A - BC) = \tfrac{1}{2}\mu_{A-BC}[v_{\mathrm{rel}}(A - BC)]^2. \tag{4}$$

For diatomic molecules in their ground electronic states, the internal energy $E_{\mathrm{int}}(BC)$ can be recast into a sum of rotational and vibrational parts: $E_{\mathrm{int}}(BC) = E_{\mathrm{rot}}(BC) + E_{\mathrm{vib}}(BC)$. The incorporation of diatomic bond dissociation energies in Eqs. (2) and (3) ensures that values of E_{int} for the various reagents and products are measured with respect to a common reference point (viz., the energy of separated neutral atoms in their ground electronic states).

Equating expressions (2) and (3) and solving for $D_0^0(\mathrm{BaI})$, one finds

$$D_0^0(\mathrm{BaI}) = D_0^0(\mathrm{HI}) + E_{\mathrm{int}}(\mathrm{BaI}) + E_{\mathrm{int}}(\mathrm{H}) - E_{\mathrm{int}}(\mathrm{Ba}) - E_{\mathrm{int}}(\mathrm{HI}) + E_{\mathrm{rel}}(\mathrm{BaI} - \mathrm{H}) - E_{\mathrm{rel}}(\mathrm{Ba} - \mathrm{HI}). \tag{5}$$

The specific conditions employed for the present investigation of BaI dissociation energies permit several of the terms in Eq. (5) to be justifiably neglected. In particular, since the $\mathrm{Ba} + \mathrm{HI}$ reaction system entails consumption and production of neutral atomic species in their ground electronic states, one finds

$$E_{\mathrm{int}}(\mathrm{Ba}) = E_{\mathrm{int}}(\mathrm{H}) = 0. \tag{6}$$

The HI utilized for our reactive studies was prepared via a well-characterized supersonic expansion that produced a translationally cold beam of $X\,^1\Sigma^+$ ground state reagent molecules. While not explicitly determined, the effective temperature for rotational and vibrational degrees of freedom in $\mathrm{HI}(X\,^1\Sigma^+)$ must lie somewhere between the stagnation temperature for the supersonic nozzle (~ 323 K) and the experimentally measured translational temperature for the beam ($\lesssim 20$ K), with values closer to the lower bound

being much more probable. For both of these limiting cases, the large vibrational spacing associated with the HI $X\,^1\Sigma^+$ potential surface ($\omega_e = 2309.01\ \text{cm}^{-1}$)[21] requires the average vibrational energy $\bar{E}_{\text{vib}}(\text{HI})$ to be essentially equal to zero. In contrast, the rotational and centrifugal distortion constants for the vibrationless level of the $X\,^1\Sigma^+$ state ($B_e = 6.4264\ \text{cm}^{-1}$, $D_e = 2.069\times10^{-4}\ \text{cm}^{-1}$)[21] yield average rotational energies of $\bar{E}_{\text{rot}}(\text{HI}) = 638$ cal/mol at 323 K and $\bar{E}_{\text{rot}}(\text{HI}) = 33.4$ cal/mol at 20 K. When compared to the uncertainties for other quantities involved in the present calculation, one is quite justified in setting $E_{\text{rot}}(\text{HI}) \approx 0$. Consequently,

$$E_{\text{int}}(\text{HI}) = E_{\text{vib}}(\text{HI}) + E_{\text{rot}}(\text{HI}) \approx 0. \tag{7}$$

By incorporating Eqs. (6) and (7) into our energy-balance arguments, a simplified expression for the dissociation energy of BaI is obtained:

$$D_0^0(\text{BaI}) = D_0^0(\text{HI}) + E_{\text{int}}(\text{BaI}) + E_{\text{rel}}(\text{BaI} - \text{H}) - E_{\text{rel}}(\text{Ba} - \text{HI}). \tag{8}$$

The experimental results derived from the present study provide a direct measure for $E_{\text{int}}(\text{BaI})$ and $E_{\text{rel}}(\text{Ba} - \text{HI})$, but yield no explicit information on $E_{\text{rel}}(\text{BaI} - \text{H})$. While the value of the product translational energy is expected to be both small[22] and constant[15,23] in the Ba + HI reaction system, the lack of any detailed knowledge for $E_{\text{rel}}(\text{BaI} - \text{H})$ proves to be the weakest link in the ensuing analysis. This difficulty can be partially mitigated by experimentally locating the most energetic quantum state populated in the nascent BaI product and assuming that the internal energy for this limiting case $E_{\text{int}}^{\text{max}}(\text{BaI})$ corresponds to a minimal partitioning of available energy into product recoil [i.e., $E_{\text{rel}}(\text{BaI} - \text{H}) \approx 0$ when the internal energy equals $E_{\text{int}}^{\text{max}}(\text{BaI})$]. The expression for $D_0^0(\text{BaI})$ can now be reformulated to give

$$D_0^0(\text{BaI}) \gtrsim D_0^0(\text{HI}) + E_{\text{int}}^{\text{max}}(\text{BaI}) - E_{\text{rel}}(\text{Ba} - \text{HI}). \tag{9}$$

The present measurements therefore provide a lower limit for the value of $D_0^0(\text{BaI})$. Note that the maximum internal energy content $E_{\text{int}}^{\text{max}}(\text{BaI})$ can be obtained in various ways depending on the differential partitioning of energy between rotational and vibrational degrees of freedom in the nascent BaI product.

III. EXPERIMENTAL

A. Overview

Figures 1 and 2 schematically illustrate the apparatus utilized in the present study. In brief, all experiments were performed with a newly constructed crossed-beam reaction chamber, in which "effusive" barium and supersonic hydrogen iodide beams intersect at 90°. Extensive use of differential pumping ensured that high-vacuum, single-collision conditions were maintained in the interaction region. A slightly supersonic beam of Ba($^1S_0$) was produced by collimating the output of a radiatively heated crucible containing barium metal. The HI($X\,^1\Sigma^+$) reagent was prepared via a skimmed and collimated supersonic expansion in various carrier gases. Changes in the nature of the carrier gas and/or the concentration of HI enabled the relative collision energy in the center-of-mass frame to be varied readily from roughly 0.1 to 0.6 eV. Reagent velocities were directly measured by means of high-resolution Doppler spectroscopy in the case of Ba($^1S_0$) and through time-of-flight (TOF) mass spectrometry in the case of HI($X\,^1\Sigma^+$). Rotational and vibrational state distributions for the nascent BaI product were deduced from high-resolution LIF spectra excited and monitored through the BaI $C\,^2\Pi$–$X\,^2\Sigma^+$ transition at 550 nm.

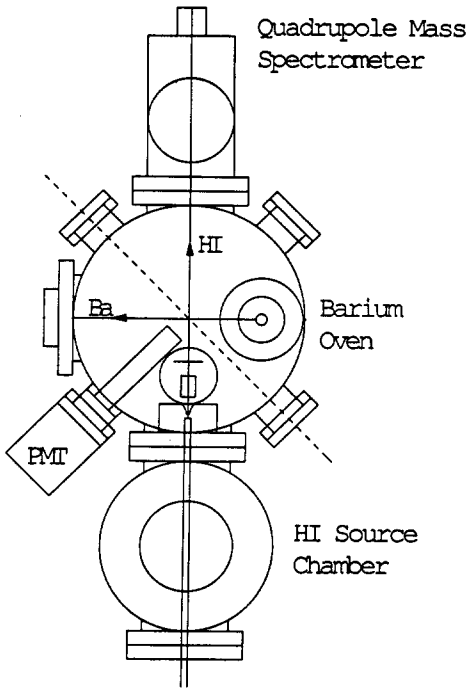

FIG. 1. A schematic diagram of the crossed-beam reaction apparatus employed for the measurement of $D_0^0(\text{BaI})$. "Effusive" Ba($^1S_0$) and supersonic HI($X\,^1\Sigma^+$) beams intersect at 90° geometry to produce BaI product molecules under well-defined, single-collision conditions.

The ensuing discussion provides a more comprehensive description for the key components of our experiment. Particular attention is directed toward the new crossed-beam reaction vessel, a high-vacuum apparatus designed specifically to generate, control, and characterize two well-collimated, high-flux sources of reagent particles. Unless otherwise stated, all reported chamber pressures were measured at ambient temperatures with uncalibrated ionization gauges.

B. Main scattering chamber

The main scattering chamber consisted of an 18 in. diameter stainless steel cylinder with *o*-ring sealed flanges providing for vacuum integrity at the upper and lower surfaces (see Fig. 1). Background pressures of $\sim 5\times10^{-8}$ Torr were achieved by evacuating the vessel with a liquid-nitrogen-baffled 6 in. diffusion pump (Varian VHS-6). This pumping system was mounted directly onto an 11 in. ASA tee piece that served to connect the main chamber to a differentially pumped quadrupole mass spectrometer utilized for HI beam analysis. A liquid-nitrogen trap located within the scattering

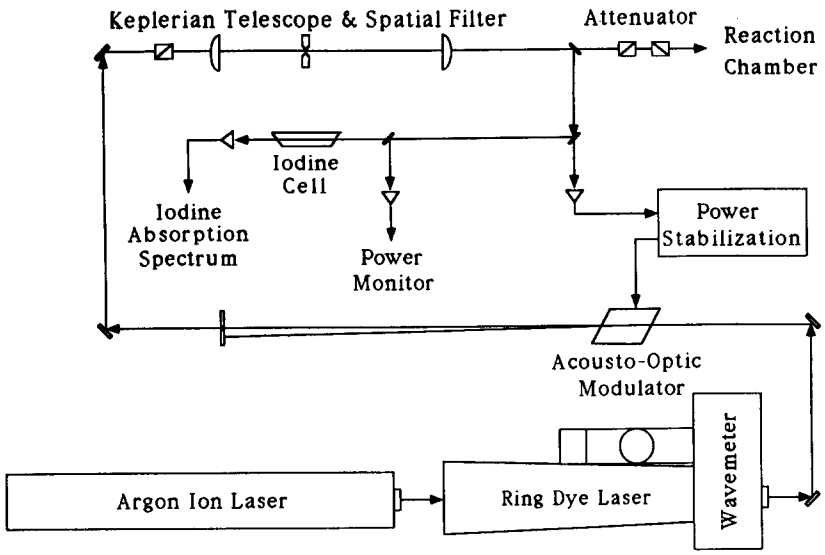

FIG. 2. A schematic diagram of the power- and frequency-stabilized cw laser source utilized for the high-resolution study of BaI product molecules.

region provided additional pumping speed for condensable reagent gases (e.g., HI). This configuration enabled the pressure to be maintained in the high 10^{-7} to low 10^{-6} Torr range under normal operating conditions.

The Ba($^1S_0$) and HI($X\,^1\Sigma^+$) sources were each collimated to yield beams of circular cross section that exhibited a nominal diameter of 1.0 cm at their point of mutual intersection (i.e., at the center of the main scattering chamber). Product molecules formed within the 0.67 cm^3 interaction volume were probed directly by means of a high-resolution laser that entered and exited through baffled arms situated on the top and bottom flanges of the scattering vessel. The resulting LIF signal was observed in an orthogonal plane through use of an optical assembly recessed into one of several metal gasket-sealed ports located about the periphery of the cylindrical main chamber.

C. HI reagent source

The HI supersonic nozzle consisted of a 100 μm diameter tantalum aperture (Ted Pella, Inc.) that had been carefully welded onto a length of tantalum tubing. Where possible, tantalum was selected as the material of choice for construction because of its superior resistance to corrosion by hydrogen halides.[24] The source assembly was designed to permit three-dimensional translation, from outside the vacuum, with respect to the 0.98 mm diameter orifice of a molecular beam skimmer (Beam Dynamics). The nozzle was typically heated to 50 °C by means of thermocoax (Amperex) tightly wrapped about the final 8 cm portion of its tip. Stagnation temperatures were regulated to $\pm$ 1 °C through a microprocessor-based controller (Omega) that utilized a metal-clad thermocouple, inserted directly into the nozzle tube, as a feedback sensor.

The chamber housing the supersonic HI source was evacuated by a water-baffled 10 in. diffusion pump (Varian VHS-10) that was backed by a two-stage mechanical pump (Sargent–Welch 1398). Liquid-nitrogen-filled cold traps were incorporated into all vacuum forelines so as to prevent the contamination and subsequent deterioration of mechanical pump fluid by the highly corrosive HI reagent. Once skimmed, the HI beam propagated through a buffer region, pumped by a water-baffled 4 in. diffusion pump (CVC PMCS-4B), which provided for differential pumping between the source and main scattering chambers. This differentially pumped region also contained a mechanical chopper that could be rotated into the beam for both TOF velocity measurements and, when desired, lock-in detection of BaI laser-induced fluorescence signal (i.e., based on phase-sensitive demodulation of the chopped Ba + HI reaction yield). Collimation of the HI source to its final half-angle of 1.18° was performed by a circular aperture located on the exit face of the buffer chamber. Typical background pressures were in the mid-10^{-8} Torr range. Under operating conditions appropriate for a mixture of 6% HI in N_2, the source and buffer chamber pressures increased to roughly 10^{-4} and 10^{-5} Torr, respectively, while pressures in the main scattering vessel remained in the high 10^{-7}–10^{-6} Torr scale.

Sample gas manipulations for the HI source were performed entirely in a custom stainless steel and tantalum manifold. This apparatus, continuously maintained at low pressures through use of a liquid-nitrogen- and molecular-sieve-trapped mechanical pump, was thoroughly baked out (at ~150 °C) prior to each experiment. Hydrogen iodide was obtained commercially (Matheson) with 98% minimum purity and subjected to several freeze–pump–thaw cycles with liquid nitrogen so as to remove residual H_2. The temperature of the HI vessel was subsequently maintained at 0 °C, in order to condense the I_2 contaminant, while a preselected quantity of hydrogen iodide vapor was permitted to enter a one-gallon reservoir (Whitey). Nitrogen (Liquid Carbonic; 99.998%) and/or helium (Liquid Carbonic; 99.995%) was then admitted to the manifold so as to prepare the desired seed-to-carrier concentration ratio (typically $\leqslant$6% HI). The long duration of individual experimental runs performed during the present study (~18 h), in con-

junction with the continuous nature of our supersonic source, required the limited volume of the reservoir to be filled to total pressures as high as 1000 psig. With the reservoir sealed off from the rest of the manifold, the enclosed gas sample was vigorously mixed through use of a magnetically coupled, teflon-coated stirring bar. The HI mixture subsequently passed through tandem single-stage regulators (Matheson), designed to maintain a preset stagnation pressure (typically $\sim$250 kPa absolute), and a 15 μm high-flow, in-line filter (Nupro) before entering the tantalum tube of the nozzle assembly.

The source configuration had a total distance from nozzle orifice to interaction region of approximately 20 cm and produced a flux of roughly 10^{17} particles cm^{-2} s^{-1} as measured for a pure beam of N_2. Mass spectrometric analysis of the HI-seeded beam revealed *no significant concentration of HI dimers*, regardless of variations in either the ionization current (0–20 mA) or the electron bombardment energy (3–100 eV) employed for creation of the measured ion signal. Possible contamination of the HI source with residual I_2 was examined through the use of high-resolution LIF spectroscopy. No evidence for this impurity was found, despite spectral searches performed over a wide range of rovibronic transitions in the I_2 $B\,^3\Pi_{0^+u}$–$X\,^1\Sigma_g^+$ system.

D. Ba reagent source

The Ba($^1S_0$) source utilized in the present study was essentially a modified version of the high-temperature oven previously described by Rettner, Wöste, and Zare.[25] A cylindrical stainless steel crucible, with a 0.8 mm diameter orifice, was filled with $\sim$60 g of barium rod (Alfa; 99.5% purity) and sealed by means of a tapered, press-fitted cap. Great care was taken to remove any residual oxide coating from the barium metal prior to its use. This greatly alleviated orifice clogging problems that were believed to stem from the presence of such refractory oxide material. Three 1/8 in. diameter ceramic rods served to support the barium-containing vessel above a water-cooled and radiatively baffled baseplate. This entire assembly was designed to be rotated and translated from outside the vacuum so as to permit fine positioning of the Ba($^1S_0$) source. Oven temperatures were measured via a W/5% Re vs W/25% Re thermocouple (Omega; type C) that was inserted through one of the supporting ceramic rods to a point within 1 mm of the crucible orifice.

The barium crucible assembly was placed into a high-temperature furnace consisting of three cylindrical layers of tantalum sheet surrounded by a water-cooled copper jacket. The tantalum functioned as a heat shield designed to contain and distribute thermal radiation within the oven. Three tungsten hairpin filaments (1.5 mm diameter), driven by a high-current/low-voltage a.c. supply so as to eliminate discharge-related formation of metastable atoms,[8] served to radiatively heat the crucible and vaporize the barium metal. Wired in parallel via a water-cooled and radiation-baffled connector block, the filaments produced the requisite operating temperature of $\sim$1320 K with input powers typically of the order of 1 kW (at 5.6 $V_{a.c.}$). A hole cut through both the tantalum heat shields and the outer water jacket enabled the resulting Ba($^1S_0$) beam to emerge from the furnace assembly. In order to minimize corrosion problems, such as those that might stem from contact with the HI reagent, all copper components of the metal atom source were electrolytically plated with nickel.

As shown in Fig. 1, the Ba($^1S_0$) source was housed in a differentially pumped, cylindrical partition that was situated directly within the confines of the main scattering chamber. This configuration ensured that the total distance from crucible orifice to interaction region was kept to a bare minimum (i.e., 10.6 cm). Evacuated by means of a water-baffled, 4 in. diffusion pump (CVC PMCS-4B), the source chamber exhibited a background pressure of roughly 10^{-8} Torr. Following an initial period of outgassing, operating pressures within this region could readily be maintained in the 10^{-6}–10^{-7} Torr range.

Before entering the main scattering chamber, the atomic beam produced by the Ba($^1S_0$) source was collimated to a half-angle of 2.82° via a custom-made set of apertures and baffles. Designed primarily with our fluorescence product detection scheme in mind, this configuration of baffles also served to trap a considerable portion of the unwanted blackbody radiation emerging from the high-temperature oven. After traversing the Ba + HI interaction region, the barium atoms impinged upon a conical catcher block that could be manually rotated into and out of the beam path. The latter position, in conjunction with a judiciously placed optical viewport and precision telescope, permitted line-of-sight alignment of the barium crucible orifice with respect to the baffle assembly. Typical Ba($^1S_0$) beam fluxes, estimated on the basis of experimentally measured velocity distributions and an assumed vapor pressure of roughly 10 Torr[26] for barium at 1320 K, were on the order of 10^{16}–10^{17} particles $cm^{-2}s^{-1}$. While not examined explicitly, barium dimerization seems to be highly unlikely due both to the mild expansion conditions employed for our "effusive" source and to the closed-shell nature of Ba($^1S_0$) atoms.

E. BaI product detection

Figure 2 illustrates the arrangement of optical components utilized in the present study. The excitation source for our LIF detection scheme was provided by a single-mode cw ring dye laser (Coherent 699-29) containing Rhodamine 560 dye (Exciton) dissolved in ethylene glycol. An integral wavemeter, in conjunction with computer-controlled frequency scanning and data acquisition, enabled high-resolution, continuous-stream spectra to be recorded over essentially the entire tuning range available to a given dye. Pumped by $\sim$6.1 W of the 5145 Å emission from a mainframe argon-ion laser (Spectra Physics 171-17), this configuration produced a peak output power in excess of 1.2 W with an actively stabilized linewidth specified to be <1 MHz. Single-frequency operation of the dye laser was continuously monitored by means of a 2 GHz scanning interferometer (Spectra Physics 470).

While the normal tuning range of the Rhodamine 560 dye was more than adequate for the majority of our BaI

studies, measurements performed on the high vibrational levels of the $C\,^2\Pi_{3/2}$–$X\,^2\Sigma^+$ $\Delta v = 0$ sequence required that the peak of the laser curve be shifted to the blue. This was accomplished by careful addition of a saturated KOH-/methanol solution to the dye mixture. Dye half-life, determined to be on the order of 150–200 watt-hours, was greatly enhanced by replacing all brass components in the commercial dye circulator with comparable parts made from stainless steel and teflon.

The dye laser power was maintained at a constant preset value ($\pm 0.5\%$; d.c. to 3 kHz bandwidth) by means of a homemade active stabilization system based on a servo-locked acousto-optic modulator (IntraAction AOM-40). The intensity of the undeflected laser beam (zero order of the AOM) was adjusted by varying the depth of modulation of the AOM grating. A Keplerian telescope/spatial filter assembly served to expand and collimate the output light, while simultaneously converting any movements in beam position, such as those that might accompany frequency scanning, into amplitude fluctuations that could subsequently be corrected for by the power stabilization loop. This optical configuration provided a source of tunable cw radiation that exhibited superior amplitude and frequency stability, as well as an exceptionally uniform Gaussian spatial profile ($\lesssim 0.8$ cm diameter). Following attenuation by a pair of polarization cubes (Karl Lambrecht), the probe light propagated through the Ba + HI interaction region in a direction perpendicular to the plane defined by the crossed reagent beams.

Spontaneous emission from the Ba + HI interaction region was collected with a custom set of $f/1.5$ optics situated in the plane of the crossed reagent beams. After being imaged onto a slit (i.e., to reject unwanted background light) and recollimated, the fluorescence was directed through a bandpass interference filter (Oriel) placed before the photocathode of a cooled photomultiplier tube (Centronic Q4283 RA at -20 °C). A set of blackened, conical baffles located in both the entrance and exit arms of the main vacuum chamber essentially eliminated any scattered laser light. Lock-in detection (PAR 124A with 116 preamplifier), based on modulation of either the probe laser or the HI source, enabled the LIF signal to be effectively discriminated from residual background noise. For the present study, the major noise source was found to entail blackbody emission from the high-temperature barium oven.

BaI excitation spectra were obtained by scanning the laser frequency under computer control (Apple IIe) while simultaneously digitizing and recording the demodulated output of the photomultiplier tube. Concurrent measurement of the I_2 absorption spectrum provided a convenient absolute frequency reference when used in conjunction with the Fourier transform atlas of Gerstenkorn and Luc.[27] In order to minimize saturation effects in the observed BaI $C\,^2\Pi$–$X\,^2\Sigma^+$ transitions, the intensity of the probe laser entering the reaction chamber was typically attenuated to less than 5 mW. The direction of linear polarization for the LIF excitation beam could be readily varied through appropriate adjustment of the optics employed in the polarization-based light attenuator.

F. Reagent velocity determination

1. HI ($X\,^1\Sigma^+$) source

The velocity distribution for HI($X\,^1\Sigma^+$) reagent was determined via standard TOF techniques.[28] In brief, roughly 15 μs pulses of the continuous HI-seeded supersonic source were produced by modulating the beam flow with a thin (0.13 mm) beryllium–copper chopper blade containing two antipodal 1 mm slits and rotating at ~ 300 Hz (TRW Globe a.c. hysteresis motor type SC). A light-emitting diode and a photodiode detector, mounted directly on the water-cooled housing of the chopper motor, served to monitor the slits' traversal of the molecular beam. The amplified and filtered signal derived from these components provided both the trigger pulse and zero time reference for the ensuing analysis.

After traversing an accurately measured flight path on the order of 75 cm, the HI pulse, now temporally broadened as a result of velocity dispersion, was ionized by electron impact and mass-selectively detected (at $m/e = 128$) by means of a differentially pumped quadrupole mass spectrometer (either a VG SX-200 or an Extrel system consisting of a 200 mm long quadrupole with 9.5 mm diameter rods). The ions were detected by a channeltron electron multiplier (Galileo) and the resulting signal was coupled into a high-speed, high-gain transimpedance amplifier (Keithley 427) before being directed to the input stage of a gated integrator-/boxcar averager (PAR 162 with 164 integrator modules). TOF spectra were obtained by utilizing a microcomputer (Apple IIe) to scan the boxcar gate repetitively over a preselected time interval, while concurrently digitizing and averaging the temporal profile of the transient HI^+ pulse. By simultaneously recording time markers from a triggerable pulse generator (HP8011A), an absolute calibration of the time scale could be readily performed.

2. Ba($^1S_0$) source

The velocity distribution for the Ba($^1S_0$) reagent was measured via the spatial properties of the Doppler effect as applied to the optical transitions of atomic barium. The probe for this analysis was provided by LIF excited through two distinct spectroscopic transitions: (1) the $^1P_1^\circ$–$^1S_0$ Ba atomic resonance line[29] at 18 060.26 cm^{-1}; and (2) the $^3D_2$–$^1S_0$ Ba two-photon transition[30] at 36 200.42 cm^{-1} (i.e., $2\times 18\,100.21$ cm^{-1}). In principle, the one-photon and two-photon spectra should provide identical information regarding the barium velocity distribution. However, in practice, the large dipole moment associated with the $^1P_1^\circ$–$^1S_0$ transition (viz., 8.02 D)[31] usually resulted in significant self-absorption of the emitted resonance radiation. The deleterious effects accompanying this radiation-trapping process[32] made the experimentally more demanding two-photon excitation scheme the method of choice for analysis of Ba($^1S_0$) velocities.

The Ba($^1S_0$) LIF was collected by the same optical imaging system and cooled photomultiplier tube used for measurement of BaI product state distributions. For the $^3D_2$–$^1S_0$ two-photon transition, individual signal photons, produced by focusing the unattenuated cw laser output

(~150 mW) through the atomic beam, were detected, amplified (Ortec 9301/474), and converted to analog form via a discriminator/ratemeter combination (Ortec 436 and 449). A narrow-bandpass interference filter (Ditric Optics), placed in front of the photomultiplier cathode, enabled selective detection of one-photon spontaneous emission through the $^3D_2$–$^3P^\circ$ transition at 440 nm. In addition to alleviating problems associated with radiation trapping, this blue fluorescence transition allowed for efficient spectral rejection of unwanted background light produced by the thermal barium source. Excitation scans, obtained by digitizing the LIF signal intensity at frequency intervals of 1 MHz, were stored on disk for later processing and analysis. Simultaneous recording of the absorption spectrum for I_2 and the reference fringes from a monitor etalon provided for absolute and relative frequency calibration, respectively.

IV. RESULTS

A. Reagent translational energies

Accurate determination of the dissociation energy for BaI requires detailed information on the relative translational energy of the colliding reagents $E_{\rm rel}$(Ba–HI). This requirement prompted a series of careful measurements designed to examine the distribution of particle velocities produced by both the Ba($^1S_0$) and HI($X\,^1\Sigma^+$) sources. Experimental results derived from these studies were subsequently interpreted in terms of a model velocity distribution $f(v)$ that was assumed to have the form

$$f(v) = (v - v_0)^2 e^{\{-[(v-v_s)/\alpha_s]^2\}}, \qquad (10)$$

where v_0, v_s, and α_s, respectively, denote the velocity offset, stream velocity, and stream width associated with a particular reactant beam. Final analysis of the velocity distributions appropriate for each reagent was based upon least-squares optimization of the v_0, v_s, and α_s parameters so as to obtain the best possible agreement between observed and calculated spectra [i.e., Doppler-limited optical spectra in the case of Ba($^1S_0$) and TOF mass spectra in the case of HI($X\,^1\Sigma^+$)]. Equation (10) was chosen not on the basis of theory, but because it provided a good fit.

The following discussion provides a more quantitative description of the velocity distributions derived for each of our reagent beams. Typical experimental results and their interpretation in terms of the model parameters in Eq. (10) are presented. In order to ensure accurate determination of the relative translation energy for the reactants, separate measurements of the Ba($^1S_0$) and HI($X\,^1\Sigma^+$) velocities were performed *during each experimental run*.

Typical $^3D_2$–$^1S_0$ two-photon LIF spectra recorded for analysis of barium velocity distributions are given in Fig. 3. Here, the first-order Doppler effect has been exploited to observe high-resolution spectra of barium under two different geometries of the laser propagation direction with respect to the Ba($^1S_0$) beam velocity. Doppler-free spectra were obtained by directing the excitation laser at 90° with respect to the collimated Ba($^1S_0$) beam. The sharp Doppler-free structure in Fig. 3 reflects the spectral shifts and hyperfine splittings associated with the naturally occurring mixture of barium isotopes.[33] The left-hand portion of Fig. 3 depicts a shifted and broadened Doppler-limited spectrum recorded with the laser intersecting the barium beam at 135°.

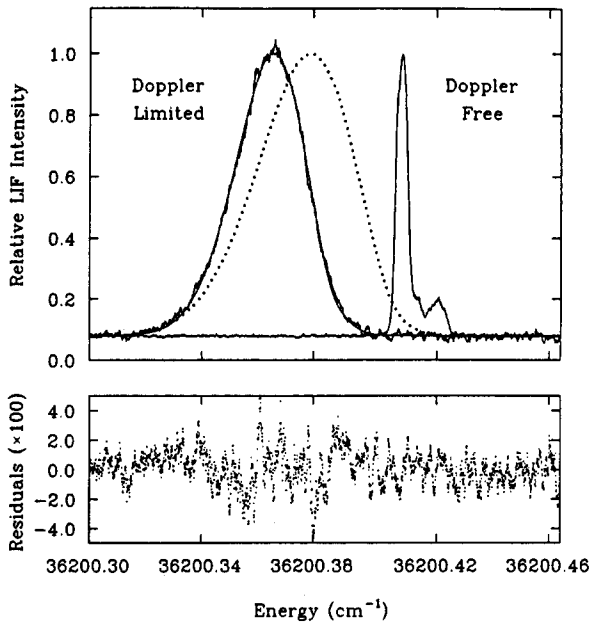

FIG. 3. Doppler spectroscopy measurements for Ba beam velocity determination. The upper panel presents high-resolution Doppler-limited and Doppler-free LIF spectra (solid curves) obtained through the Ba $^3D_2$–$^1S_0$ two-photon transition. Also shown are simulated Doppler-limited profiles corresponding to a Maxwell–Boltzmann distribution of velocities at the temperature (1320 K) of the oven crucible (dotted curve) and to the best fit of Eq. (10) to the experimental data (smooth solid curve). The model velocity parameters and their 1σ uncertainties are $v_0 = 262(4)$ m s^{-1}, $v_s = 267(33)$ m s^{-1}, and $\alpha_s = 284(15)$ m s^{-1}. Associated residuals are presented in the lower panel.

Convolution of the Doppler-free spectrum with an appropriate form for the barium velocity distribution should yield a simulation of the Doppler-limited results.[34] Initial attempts to represent the barium velocities in terms of a Maxwell–Boltzmann distribution, with the temperature set equal to that of our oven crucible, produced the Doppler-limited spectrum denoted by dotted lines in Fig. 3. Obviously, this simple model for $f(v_{\rm Ba})$, which is quite appropriate for an effusive beam emerging from a thermal source, provides an inadequate description of the present experimental conditions.

The supersonic expansion formula embodied in Eq. (10) was found to provide a much more satisfactory description for the distribution of barium velocities emerging from our nominally effusive source. A simulated Doppler-limited spectrum, resulting from nonlinear least-squares optimization[35] of the model velocity parameters contained in $f(v_{\rm Ba})$, is shown in Fig. 3. The width of the measured velocity distribution, which corresponds to a translational temperature of roughly 670 K, is clearly narrower than that associated with a thermal source at the 1320 K temperature of the barium crucible.

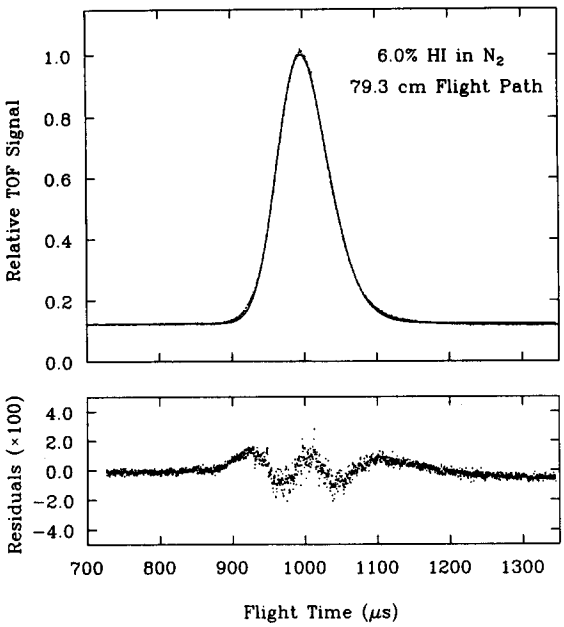

FIG. 4. Time-of-flight measurements for HI beam velocity determination. The upper panel depicts the experimental TOF signal (dots) and the simulation of the best fit of Eq. (10) to the experimental data (solid curve). The model velocity parameters and their 1σ uncertainties are $v_s = 757.2(14)$ m s^{-1} and $\alpha_s = 36.3(9)$ m s^{-1}. Associated residuals are presented in the lower panel.

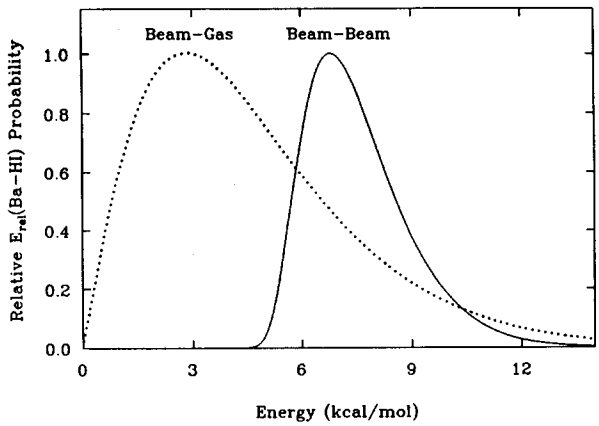

FIG. 5. The distribution of reagent translational energies E_{rel}(Ba–HI) (solid curve) associated with the crossed-beam determination of BaI dissociation energies. From this curve, it is determined that $\overline{E}_{rel}$(Ba–HI) = 7.54 kcal/mol, E^*_{rel}(Ba–HI) = 6.78 kcal/mol, and $\sigma_{E_{rel}}$(Ba–HI) = 1.43 kcal/mol. The dotted curve denotes the translational energy spread reported for a previous beam-gas study of the Ba + HI reaction (Ref. 14).

Figure 4 presents a typical TOF spectrum recorded for analysis of HI velocity distributions. The actual experimental data, denoted by individual dots, were obtained by digitizing the time-resolved output of an rf quadrupole filter that had been tuned to $m/e = 128$ so as to monitor the mechanically chopped beam from our HI($X\,^1\Sigma^+$) supersonic source. While the signal arrival time provides a crude estimate for the average HI velocity, the broadened temporal profile of the pulse contains detailed information on the overall shape of the HI velocity distribution. The results shown in Fig. 4 correspond to a mixture of ~6.0% HI in nitrogen carrier gas with the stagnation pressure and nozzle temperature maintained at 251 kPa and 50 °C, respectively. These conditions are representative of those employed for the present study of BaI dissociation energies.

Analysis of the translational energy spread associated with the supersonic HI($X\,^1\Sigma^+$) source was based upon direct numerical simulation of the experimental TOF spectra.[28] This procedure entailed convolution of a parametrized distribution for HI velocities [Eq. (10)] with temporal functions describing the traversal of the chopper slit across the molecular beam and the overall response time of our apparatus. Values of parameters incorporated into the velocity model were optimized, by means of a nonlinear least-squares regression algorithm,[35] so as to obtain the best possible agreement between the observed and calculated TOF profiles. The accurate determination of HI velocities demanded that all recorded flight times be corrected by subtraction of the experimentally measured mass- and charge-dependent transit times for ions within the quadrupole mass spectrometer.

The solid curve in Fig. 4 represents the numerical simulation for the experimental TOF spectrum as derived from our least-squares regression procedure. Optimized values for the v_s and α_s parameters, as well as their associated one-standard-deviation confidence limits, are presented in the caption. Since the velocity offset v_0 of Eq. (10) could not be uniquely determined as an independent variable, its value has been set equal to zero for the HI beam analysis. The exceptionally narrow width of the deconvoluted HI velocity distribution, corresponding to a translational temperature of roughly 20 K, confirms the supersonic nature of the HI($X\,^1\Sigma^+$) reagent source.

Figure 5 depicts the distribution of reagent translational energies, E_{rel}(Ba–HI), associated with the present set of experimental conditions. This plot was derived from the independently measured velocity functions for the Ba($^1S_0$) and HI($X\,^1\Sigma^+$) reactant beams by converting them to a relative (i.e., center-of-mass) coordinate frame and numerically convoluting them together subject to the constraints imposed by the 90° crossing geometry of our reaction apparatus.[20] The mean [$\overline{E}_{rel}$(Ba–HI)], most probable [E^*_{rel}(Ba–HI)], and standard deviation [$\sigma_{E_{rel}}$(Ba–HI)] for the calculated translational energy distribution are given in the caption.

The dotted curve in Fig. 5 represents the translational energy distribution reported in a recent beam-gas investigation of the Ba + HI reaction system.[14] It is particularly important to note that the spread in our crossed-beam E_{rel}(Ba–HI) distribution, corresponding to a $\sigma_{E_{rel}}$(Ba–HI)/$\overline{E}_{rel}$(Ba–HI) ratio of roughly 18%, is over a factor of 2 narrower than that associated with the previous beam-gas study. The energy uncertainty arising from the range of E_{rel}(Ba–HI) values available to the reagents constitutes the major source of nonsystematic error for the determination of D^0_0(BaI).

It must be stressed that the results presented in Fig. 5 actually reflect the spread in translational energy available

for *colliding* reagents, not necessarily for *reacting* reagents. While indicating the probability for bimolecular collisions to occur with a given relative energy, the shape determined for the E_{rel} (Ba–HI) distribution does not reveal whether or not the colliding species react or, moreover, what final product states are formed. In the absence of any additional information, the analysis assumes that Fig. 5 roughly corresponds to the distribution of E_{rel} (Ba–HI) for reactive encounters. The implications of this assumption, especially with regards to the uncertainties placed on our calculated value of D_0^0(BaI), will be discussed below.

B. BaI product state analysis

Figure 6 presents a high-resolution LIF spectrum obtained by scanning the frequency of our probe laser through the entire BaI $C\,^2\Pi_{3/2}$–$X\,^2\Sigma^+$ $\Delta v = 0$ band system while simultaneously monitoring the undispersed fluorescence signal originating from the nascent BaI product molecules. The crossed-beam conditions employed for this measurement are completely specified by the distribution of reagent translational energies reported in the preceding section. Although the actual experimental data might appear to be somewhat noisy, closer inspection reveals this to be primarily a consequence of individual rovibronic transitions resolved by the single-mode cw excitation laser. When compared and contrasted with results derived from previous beam-gas studies,[11,14] the spectrum in Fig. 6 immediately reveals significant differences in rotation–vibration population distributions for the BaI product. These variations and their implications for the determination of D_0^0(BaI) form the basis for the ensuing discussion.

In order to extract a value for D_0^0(BaI) from our LIF measurements, the populated quantum states of the BaI product must be identified and characterized as to their internal energy content. A thorough understanding of BaI spectroscopy is essential for any such undertaking. Despite considerable efforts expended by several research groups,[11,19,36–39] a complete rovibronic assignment for the

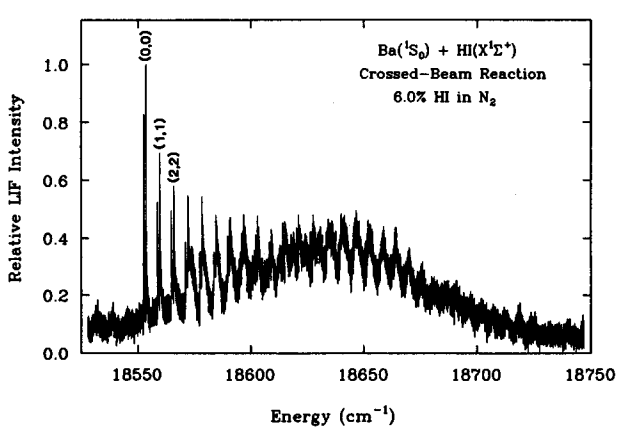

FIG. 6. A high-resolution LIF spectrum spanning the entire BaI $C\,^2\Pi_{3/2}$–$X\,^2\Sigma^+$ $\Delta v = 0$ band system. The features revealed by this long-range scan reflect the rotational and vibrational population distributions in the nascent BaI product molecules. The $P_{21}(J)$, $Q_2(J)$ double bandheads for the lowest (v,v) vibronic transitions are labeled.

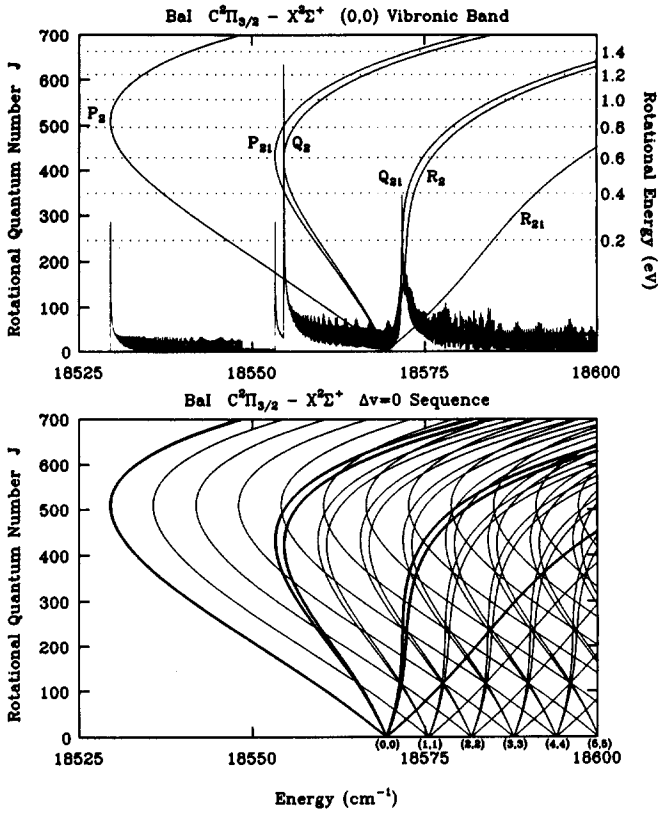

FIG. 7. Rovibronic spectroscopy of BaI as observed through the $C\,^2\Pi_{3/2}$–$X\,^2\Sigma^+$ $\Delta v = 0$ band system. The upper panel depicts a detailed Fortrat diagram for the (0,0) vibronic transition with a superimposed spectral simulation obtained by equally populating all rotational levels up to $J = 700.5$. The lower panel demonstrates the spectral congestion arising from overlapping vibronic structure within the $\Delta v = 0$ sequence.

entire BaI C–X system still remains a quite formidable task. In part, the difficulties associated with analysis of the C–X transition stem from the small, nearly equal rotational constants for the C and X states ($B \sim 0.027$ cm^{-1}),[19] which, in conjunction with the presence of six distinct rotational branches per subband, lead to the formation of exceptionally congested vibronic bands. This problem is succinctly illustrated by the upper panel of Fig. 7, which shows a detailed Fortrat diagram and superimposed spectral simulation for the BaI $C\,^2\Pi_{3/2}$–$X\,^2\Sigma^+$ (0,0) band, as derived from work performed in this laboratory.[19,40] Furthermore, the nature of the C–X transition,[41] which involves the transfer of an electron between two nonbonding molecular orbitals centered primarily on the Ba atom, means that the upper state potential surface is essentially identical, both in shape and equilibrium internuclear distance, to that of the ground state. Therefore, Franck–Condon factors strongly favor $\Delta v = 0$ vibronic transitions that, in turn, are separated in frequency only by the relatively small difference in vibrational constants between the C and X states (viz., $\omega_e^{\Pi} - \omega_e^{\Sigma} \sim 6.2$ cm^{-1}).[42,43] As depicted in the lower panel of Fig. 7, this results in a closely spaced sequence of (v,v) Fortrat parabolas with the density of rovibronic transitions rapidly approaching several hundred per wavenumber.

As suggested by Fig. 7, the overall band contours corre-

sponding to individual vibronic transitions within the BaI C–X system can furnish some indication as to the internal energy content of our product molecules. Provided that sufficient rotational excitation is present, the rotational and centrifugal distortion constants for the (0,0) band lead to the formation of three blue-shaded bandheads: two closely spaced "double" bandheads at $J\sim427.5$, where $E_{\rm rot}$(BaI)$\approx$0.60 eV [derived from $P_{21}(J)$ and $Q_2(J)$ transitions] and one far-displaced "high-J" bandhead at $J\sim508.5$, where $E_{\rm rot}$(BaI)$\approx$0.84 eV [derived from $P_2(J)$ transitions]. It should be noted that 0.60 and 0.84 eV of rotational excitation in vibrationless BaI $X\,^2\Sigma^+$ is approximately isoenergetic with the rotationless levels of $v=34$ and $v=49$, respectively! Assuming that the relative values of spectroscopic constants for the C and X states are roughly independent of vibrational quantum numbers, the presence of bandhead feature in the LIF spectra provide a direct indication for the degree of rotational excitation associated with individual product vibrational states.

In light of the (0,0) Fortrat diagram, the sharp "doublet" features in the low-frequency region (viz., near 18 560 $\rm cm^{-1}$) of Fig. 6 can now be attributed to the formation of closely spaced $P_{21}(J)$ and $Q_2(J)$ bandheads for the lowest $\Delta v=0$ vibronic bands. However, under the present experimental conditions, insufficient product rotational excitation exists for the creation of "high-J" $P_2(J)$ bandheads.[44] Nevertheless, clusters of spectral lines, corresponding to individual rovibronic transitions within the $P_2(J)$ branch, can be readily identified for the first few vibrational states in the vicinity of 18 535 $\rm cm^{-1}$. The presence of $P_{21}(J)$ and $Q_2(J)$ bandheads and the absence of $P_2(J)$ bandheads immediately place lower and upper bounds on the maximum degree of BaI rotational excitation, namely, $4800\lesssim E_{\rm rot}^{\rm max}({\rm BaI})\leqslant 6775$ $\rm cm^{-1}$. In the case of vibrationless BaI, these limiting values for rotational excitation must also equal the maximum amount of internal energy contained within the nascent product molecules $E_{\rm int}^{\rm max}$ (BaI). Assuming that bandhead formation is not affected significantly by changes in vibrational quantum numbers and noting that the "double" $P_{21}(J)$, $Q_2(J)$ bandheads seems to disappear after $v\approx6$, where $E_{\rm vib}({\rm BaI})=901$ $\rm cm^{-1}$, a more refined estimate of $E_{\rm rot}^{\rm max}({\rm BaI})\leqslant 5700$ $\rm cm^{-1}$ can be deduced from our LIF measurements.

With increasing BaI vibrational excitation, the sharp double bandheads in Fig. 6 are supplanted by a regular pattern of slowly modulating spectral intensity. These features, separated in frequency by roughly the 6.2 $\rm cm^{-1}$ difference in vibrational constants between the C and X states, can be attributed to dense $C\,^2\Pi_{3/2}$–$X\,^2\Sigma^+(v,v)$ rovibronic structure derived from low rotational excitation (i.e., $J\leqslant300$) of individual BaI $X\,^2\Sigma^+$ vibrational levels. Previous studies[11,19,37,38] based upon low-resolution spectroscopic probes ascribed oscillations analogous to those depicted in the central portion of Fig. 6 to the formation of $\Delta v=0$ bandheads. A more detailed analysis of high rotational levels in the (0,0) vibronic band,[40] made possible by our use of crossed-beam reaction conditions and high-resolution LIF spectroscopy, suggests that this is not the case. In particular, as shown by Fig. 7, the low-J inflection points in the $Q_{21}(J)$ and $R_2(J)$ branches can lead to a sharp local region of spectral congestion that resembles a true bandhead.

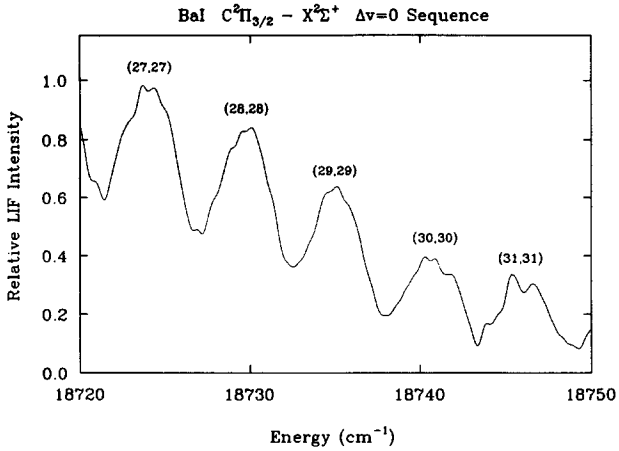

FIG. 8. The expanded portion of the BaI $C\,^2\Pi_{3/2}$–$X\,^2\Sigma^+(v,v)$ LIF spectrum in a region corresponding to population of highly excited vibrational levels. Gross numerical smoothing of the experimental data reveals the band contours for individual $\Delta v=0$ vibronic transitions.

Since Franck–Condon factors for individual $\Delta v=0$ bands in the BaI C–X system are all approximately equal to unity,[11,12,41] the LIF spectrum of Fig. 6 suggests that the BaI $X\,^2\Sigma^+$ product formed in our crossed-beam study is highly vibrationally excited, exhibiting an inverted vibrational distribution that is bell shaped with a peak near $v\approx12$. For the lowest vibrational levels, the unusually large intensity associated with the $P_{21}(J)$,$Q_2(J)$ double bandheads reflects the selective population of a narrow range of rotational states (viz., $J\sim427.5$) as dictated by the influence of kinematic constraints in the Ba + HI reaction.[3,14,15] Note that these sharp bandhead features, which totally dominate the observed LIF spectra, form roughly 15 $\rm cm^{-1}$ to the red of the corresponding vibronic origin (cf., Fortrat diagram in Fig. 7).

Figure 8 shows an expanded portion of the BaI LIF spectrum attributed to $\Delta v=0$ transitions from highly excited $X\,^2\Sigma^+$ vibrational levels. Here, gross numerical smoothing of the experimental data has been performed so as to reveal the overall contours for individual vibronic bands. Definitive assignments for each (v,v) transition are displayed above the corresponding spectral feature. The gradual decrease in spectral intensity with increasing degree of vibrational excitation reflects the diminishing population of the higher $X\,^2\Sigma^+$ vibrational levels in the nascent BaI product.

Analysis and extrapolation of LIF spectra recorded for (v,v) vibronic transitions beyond those depicted in Fig. 8 suggest that the highest-lying $X\,^2\Sigma^+$ vibrational state populated under the present experimental conditions is $v=34$ with an uncertainty of two vibrational quanta. This extrapolation is more difficult than Fig. 8 suggests because of interfering contributions from the $\Delta v=+1$ sequence. Assuming that rotational excitation within this limiting vibrational level is negligible, our best estimate for the maximum inter-

nal energy content of the nascent BaI product molecules is given by $E_{\rm int}^{\rm max}({\rm BaI}) \approx E_{\rm vib}^{\rm max}({\rm BaI}) = 4850 \pm 300\ {\rm cm}^{-1}$, where we have used $\omega_e^{\Sigma} = 152.140\ {\rm cm}^{-1}$ and $\omega_e^{\Sigma} x_e^{\Sigma} = 0.2746\ {\rm cm}^{-1}$.[42] It must be stressed that the observation of an energetic cutoff at $v \approx 34$ via the $C\,^2\Pi_{3/2}$–$X\,^2\Sigma^+$ $\Delta v = 0$ band system is not influenced by the onset of predissociation in the excited electronic state, which has been reported to occur near $v \approx 62$ by Johnson, Allison, and Zare.[13] Note that the value of $E_{\rm int}^{\rm max}({\rm BaI})$ deduced from vibrational populations is consistent with the upper limit suggested earlier from rotational bandhead features.

C. Calculation of lower bound for D_0^0(BaI)

With the maximum internal energy content of BaI determined to be $E_{\rm int}^{\rm max}({\rm BaI}) = 13.87 \pm 0.86$ kcal/mol on the basis of the highest observed product vibrational state, the energy-balance arguments embodied in Eq. (9) can now be invoked for the calculation of $D_0^0({\rm BaI})$. The mean value and standard deviation for the experimentally measured distribution of relative reagent translational energies (cf., Fig. 5) indicate that $\overline{E}_{\rm rel}({\rm BaI–H}) = 7.54 \pm 1.43$ kcal/mol. Therefore, given the well-known bond dissociation energy for HI [viz., $D_0^0({\rm HI}) = 70.429 \pm 0.025$ kcal/mol],[21,45] one finds

$$D_0^0({\rm BaI}) \gtrsim 76.8 \pm 1.7\ {\rm kcal/mol}, \qquad (11)$$

where the error bar reflects independent propagation of the uncertainties associated with the individual terms of Eq. (9).

The large spread in the translational energy distribution of Fig. 5 provides the major source of statistical uncertainty for the present analysis. In addition, no information exists as to what portion of the measured distribution is reactive and, more importantly for our analysis, what portion leads to the population of high vibrational states in the nascent BaI product molecules. Consequently, both the explicit neglect of product recoil energy $E_{\rm rel}$(BaI–H) and the implicit assumption that all reagent collisional energies result in the formation of highly vibrationally excited BaI furnish possible sources of systematic error for the bond dissociation measurements. It must be stressed, however, that our *lower limit* for D_0^0(BaI) and its associated error bar are thought to more than encompass any reasonable estimates for these uncertainties.

V. DISCUSSION

Table I contains a compilation of the results derived from attempts to determine the bond dissociation energy of BaI. Where available, the error bars and bounds associated with each measurement have been indicated. The exoergicity for the $Ba(^1S_0) + HI(X\,^1\Sigma^+) \rightarrow BaI(X\,^2\Sigma^+) + H(^2S_{1/2})$ reaction system, defined by $\Delta E = D_0^0({\rm BaI}) - D_0^0({\rm HI})$, has also been tabulated for each of the reported values of D_0^0(BaI).

At first glance, the chronologically ordered listing of Table I reveals a large disparity among the reported bond dissociation energies for BaI, with the correlated energetics for the Ba + HI reaction system ranging from somewhat endoergic to extremely exoergic. However, upon closer inspection, most of the previously measured values of D_0^0(BaI) are in the vicinity of ~72 kcal/mol. The one exception, an early chemiluminescence study of Dickson, Kinney, and Zare,[7] which yielded a value of 102 kcal/mol, must be discounted due to contamination of their barium source by electronically excited atoms.[8] It is particularly interesting to note that the roughly 28 kcal/mol discrepancy, which differentiates the results of Dickson and co-workers from the other measurements, is in excellent agreement with the energy required for the formation of metastable $Ba(^3D)$ from ground state barium.[46]

Aside from the early molecular beam scattering studies of Mims, Lin, and Herm,[6] which provide a lower limit for D_0^0(BaI) of 66 kcal/mol, the remaining bond dissociation energies of Table I are all in relatively close proximity to the lower bound of 76.8 ± 1.7 kcal/mol derived from the present work. However, in light of our experimental observations, the few kcal/mol discrepancies that do exist are quite significant. On the basis of equilibrium thermochemical data obtained through high-temperature mass spectrometric measurements, Kleinschmidt and Hildenbrand[9] have con-

TABLE I. Compilation of bond dissociation energies measured for BaI. The corresponding exoergicity of the $Ba(^1S_0) + HI(X\,^1\Sigma^+) \rightarrow BaI(X\,^2\Sigma^+) + H(^2S_{1/2})$ reaction, defined by $\Delta E = D_0^0({\rm BaI}) - D_0^0({\rm HI})$, is also indicated.

Investigator	Method	D_0^0(BaI) (kcal/mol)	ΔE (kcal/mol)
Mims, Lin, and Herm[a]	Molecular beam scattering	$\geqslant 66$	$\geqslant -4.4$
Dickson, Kinney, and Zare[b]	Chemiluminescence	102 ± 1	$+31.6$
Kleinschmidt and Hildenbrand[c]	Mass spectrometry	71.4 ± 1.0	$+1.0$
Estler and Zare[d]	Chemiluminescence	72.9 ± 2	$+2.5$
Johnson, Allison, and Zare[e]	Predissociation	$\leqslant 78.5 \pm 0.5$	$\leqslant +8.1$
This work	LIF	$\geqslant 76.8 \pm 1.7$	$\geqslant +6.4$

[a] Reference 6.
[b] Reference 7.
[c] Reference 9.
[d] Reference 8.
[e] Reference 13.

cluded that $D_0^0(\mathrm{BaI}) = 71.4 \pm 1.0$ kcal/mol. To assess this value, Eq. (9) can be solved for the maximum internal energy content of the nascent BaI product:

$$E_{\mathrm{int}}^{\mathrm{max}}(\mathrm{BaI}) \lesssim D_0^0(\mathrm{BaI}) - D_0^0(\mathrm{HI}) + E_{\mathrm{rel}}(\mathrm{Ba\text{–}HI}). \tag{12}$$

By utilizing the mean relative translational energy measured for our experimental conditions [viz., $\bar{E}_{\mathrm{rel}}(\mathrm{Ba\text{–}HI}) = 7.54 \pm 1.43$ kcal/mol] in conjunction with the known dissociation energy for HI, the $D_0^0(\mathrm{BaI})$ value suggested by Kleinschmidt and Hildenbrand yields $E_{int}^{\mathrm{max}}(\mathrm{BaI}) \lesssim 8.5 \pm 1.7$ kcal/mol. This upper bound for the internal energy content of BaI is barely enough to populate $v = 20$ and is insufficient to lead to formation of the $P_{21}(J)$,$Q_2(J)$ double bandheads observed for the $C\,^2\Pi_{3/2}$–$X\,^2\Sigma^+$ (0,0) vibronic transition (cf., Fig. 7). Even after taking the rather conservative error bar into account, such that $E_{int}^{\mathrm{max}}(\mathrm{BaI}) \lesssim 10.2$ kcal/mol, only vibrational levels lower than $v \approx 25$ would be formed with the vibrationless level still not exhibiting any bandhead features. Obviously these conclusions contradict the spectroscopic observations made during our crossed-beam measurements. Given that the values of $D_0^0(\mathrm{CaF})$ and $D_0^0(\mathrm{SrF})$ derived by the same authors via identical mass-spectrometric methods [9] are in excellent agreement with the bond dissociation energies obtained through application of energy-balance arguments to the Ca + HF($v = 1$) and Sr + HF($v = 1$) reaction systems,[47] the apparent discrepancy between our results and the BaI dissociation energy reported by Kleinschmidt and Hildenbrand[9] is quite perplexing. Hopefully, this problem will be resolved in the near future. Since a first draft of this manuscript was prepared, Hildenbrand has informed us that recent work with Lau in his laboratory has provided a revised value of $D_0^0(\mathrm{BaI}) = 76.2 \pm 2$ kcal/mol based on several independent reaction systems including the dissociation equilibrium BaI(g) = Ba(g) + I(g) in which the temperature dependence of the equilibrium constant was measured.[48]

While less dramatic in its shortcomings, the BaI bond strength derived from the chemiluminescence studies of Estler and Zare[8] also seems to be somewhat low. These authors utilized a discharge to prepare metastable barium atoms and interpreted their results in terms of the Ba(^3D) + I_2 reaction system. However, unavoidable formation of metastable Ba(^1D) in their source might have contributed to the observations reported by Estler and Zare. Since the ^1D level of barium is located roughly 2115 cm^{-1} above Ba(^3D),[46] reinterpretation of the chemiluminescence data suggests a bond dissociation energy of $D_0^0(\mathrm{BaI}) \geqslant 78.9 \pm 2$ kcal/mol, a value in reasonably good agreement with that derived from the present study.

In a recent study of the Ba + $CF_3I \rightarrow$ BaI + CF_3 reaction system, Johnson, Allison, and Zare[13] have found evidence for predissociation in the $C\,^2\Pi$ electronically excited state of BaI. Based on the sudden loss of observed LIF signal intensity, as well as on rapid variations in effective rotational constants and vibrational spacings, these authors concluded that the onset of predissociation occurs at $v \sim 62$ and $v \sim 78$ in the $\Omega = 3/2$ and $\Omega = 1/2$ spin–orbit components, respectively. Since the repulsive curves responsible for these nonadiabatic perturbations must correlate to the same asymptotic separated-atom limit as the $X\,^2\Sigma^+$ ground potential, predissociation of the C state establishes an upper bound of

$$D_0^0(\mathrm{BaI}) \leqslant 78.5 \pm 0.5 \text{ kcal/mol}. \tag{13}$$

The lower bond for the BaI bond dissociation energy deduced from our crossed-beam measurements falls roughly 1.6 kcal/mol below this upper limit. We therefore recommend a value of

$$D_0^0(\mathrm{BaI}) = 77.7 \pm 2.0 \text{ kcal/mol} \tag{14}$$

for the bond strength of BaI. The error bar has been chosen essentially to encompass the range of uncertainties suggested by Eqs. (11) and (13).This new value of $D_0^0(\mathrm{BaI})$ implies an exoergicity of $\Delta E = 7.3 \pm 2.0$ kcal/mol for the Ba($^1S_0$) + HI($X\,^2\Sigma^+$) reaction. By exploiting a full rotational analysis for the product state distributions, in conjunction with the constraints on angular momentum disposal imposed by the kinematic or mass-dependent effects that govern the Ba + HI system,[3] an even more refined estimate for the BaI bond dissociation energy should be possible.

ACKNOWLEDGMENTS

The authors wish to thank C. Noda for useful discussions and technical assistance and C. R. Dickson for assistance in obtaining some of the equipment. P.H.V. thanks the IBM Corporation for support through a postdoctoral fellowship. C.A.L. thanks the Lindemann Trust for a postdoctoral fellowship. W.E.E. thanks the Deutsche Forschungsgemeinschaft for a Heisenberg Fellowship. This work was supported by the National Science Foundation under Grant No. NSF CHE 89-21198.

[1] A. G. Gaydon, *Dissociation Energies and Spectra of Diatomic Molecules*, 3rd ed. (Chapman and Hall, London, 1968).
[2] R. N. Zare, Ber. Bunsenges. Phys. Chem. **78**, 153 (1974).
[3] P. H. Vaccaro, A. A. Tsekouras, D. Zhao, C. A. Leach, and R. N. Zare (in preparation).
[4] E. S. Rittner, J. Chem. Phys. **19**, 1030 (1951).
[5] K. S. Krasnov and N. V. Karaseva, Opt. Spectrosc. **19**, 14 (1965).
[6] C. A. Mims, S.-M. Lin, and R. R. Herm, J. Chem. Phys. **57**, 3099 (1972).
[7] C. R. Dickson, J. B. Kinney, and R. N. Zare, Chem. Phys. **15**, 243 (1976).
[8] R. C. Estler and R. N. Zare, Chem. Phys. **28**, 253 (1978).
[9] P. D. Kleinschmidt and D. L. Hildenbrand, J. Chem. Phys. **68**, 2819 (1978).
[10] D. L. Hildenbrand, J. Chem. Phys. **66**, 3526 (1977).
[11] H. W. Cruse, P. J. Dagdigian, and R. N. Zare, Faraday Discuss. Chem. Soc. **55**, 277 (1973).
[12] P. J. Dagdigian, H. W. Cruse, and R. N. Zare, Chem. Phys. **15**, 249 (1976).
[13] M. A. Johnson, J. Allison, and R. N. Zare, J. Chem. Phys. **85**, 5723 (1986).
[14] C. Noda, J. S. McKillop, M. A. Johnson, J. R. Waldeck, and R. N. Zare, J. Chem. Phys. **84**, 856 (1986).
[15] C. Noda and R. N. Zare, J. Chem. Phys. **86**, 3968 (1987).
[16] R. B. Bernstein and B. E. Wilcomb, J. Chem. Phys. **67**, 5809 (1977).
[17] G. P. Smith, J. C. Whitehead, and R. N. Zare, J. Chem. Phys. **67**, 4912 (1977).

[18]M. A. Johnson, C. W. Webster, and R. N. Zare, J. Chem. Phys. **75**, 5575 (1981).
[19]M. A. Johnson, C. Noda, J. S. McKillop, and R. N. Zare, Can. J. Phys. **62**, 1467 (1984); M. A. Johnson and R. N. Zare, J. Chem. Phys. **82**, 4449 (1985).
[20]S. Datz, D. R. Herschbach, and E. H. Taylor, J. Chem. Phys. **35**, 1549 (1961).
[21]K. P. Huber and G. Herzberg, *Molecular Spectra and Molecular Structure. IV. Constants of Diatomic Molecules* (Van Nostrand-Reinhold, New York, 1979).
[22]The potential surface governing the Ba + HI system is expected to exhibit an early barrier that channels most of the reaction exoergicity into product internal excitation rather than product recoil. See M. H. Mok and J. C. Polanyi, J. Chem. Phys. **51**, 1451 (1969).
[23]A. Siegel and A. Schultz, J. Chem. Phys. **76**, 4513 (1982).
[24]W. Braker and A. L. Mossman, *Matheson Gas Data Book* (Matheson Gas Products, Secaucus, N.J., 1980).
[25]C. T. Rettner, L. Wöste, and R. N. Zare, Chem. Phys. **58**, 371 (1981).
[26]H. Hartmann and R. Schneider, Z. Anorg. Allgem. Chem. **180**, 275 (1929); Ind. Eng. Chem. **39**, 517 (1947); *CRC Handbook of Chemistry and Physics* (CRC, Boca Raton, 1984).
[27]S. Gerstenkorn and P. Luc, *Atlas du Spectre d'Absorption de la Molecule d'Iode* (Centre National de la Recherche Scientifique, Paris, 1978); S. Gerstenkorn and P. Luc, Rev. Phys. Appl. **14**, 791 (1979).
[28]D. J. Auerbach, in *Atomic and Molecular Beam Methods*, edited by G. Scoles (Oxford University, New York, 1988), Vol. 1.
[29]P. E. G. Baird, R. J. Brambley, K. Burnett, D. N. Stacey, D. M. Warrington, and G. K. Woodgate, Proc. R. Soc. London Ser. A **365**, 567 (1979).
[30]W. Jitschin and G. Meisel, Z. Phys. A **295**, 37 (1980).
[31]S. Niggli and M. C. E. Huber, Phys. Rev. A **39**, 3924 (1989).
[32]C. J. Cannon, *The Transfer of Spectral Line Radiation* (Cambridge University, Cambridge, 1985).
[33]$_{56}Ba^{138}$, the most prevalent isotope of barium at 71.66% natural abundance, has a nuclear spin of zero and, therefore, no hyperfine structure. While the largest peak in the Doppler-free spectra of Fig. 3 does correspond to $_{56}Ba^{138}$, the contribution of other, less abundant isotopes has been grossly exaggerated by the detection geometry utilized in our LIF excitation scheme.
[34]U. Hefter and K. Bergmann, in *Atomic and Molecular Beam Methods*, edited by G. Scoles (Oxford University, New York, 1988), Vol. 1.
[35]D. W. Marquardt, J. Soc. Ind. Appl. Math. **11**, 431 (1962).
[36]M. A. Johnson and R. N. Zare, J. Chem. Phys. **82**, 4449 (1985).
[37]P. Mesnage, Ann. Phys. (Paris) **11**, 5 (1939).
[38]M. M. Patel and N. R. Shah, Indian J. Pure Appl. Phys. **8**, 681 (1970).
[39]W. E. Ernst, J. Kändler, C. Noda, J. S. McKillop, and R. N. Zare, J. Chem. Phys. **85**, 3735 (1986).
[40]D. Zhao, P. H. Vaccaro, A. A. Tsekouras, C. A. Leach, and R. N. Zare (in preparation).
[41]P. J. Dagdigian, H. W. Cruse, and R. N. Zare, J. Chem. Phys. **60**, 2330 (1974).
[42]T. Törring and K. Döbl, Chem. Phys. Lett. **115**, 328 (1985).
[43]M. L. P. Rao, D. V. K. Rao, R. T. Rao, and P. S. Murty, Fizika **9**, 25 (1977).
[44]The absence of "high-J" bandhead features in Fig. 6 has been demonstrated by seeding the HI reagent in helium carrier gas rather than nitrogen. The higher translational energies afforded by these experimental conditions permit direct identification and assignment of the $P_2(J)$ bandheads.
[45]The error bar placed on the HI bond dissociation energy reflects the spread of $D_0^0(\mathrm{HI})$ values calculated from various thermochemical measurements.
[46]C. E. Moore, *Atomic Energy Levels* (National Bureau of Standards, Washington, D.C., 1971), Vol. 3.
[47]Z. Karny and R. N. Zare, J. Chem. Phys. **68**, 3360 (1978).
[48]D. L. Hildenbrand (private communication).